ELSEVIER

Journal of Electron Spectroscopy and Related Phenomena 96 (1998) 53–60

JOURNAL OF ELECTRON SPECTROSCOPY and Related Phenomena

Structural studies of WC(0001) and the adsorption of benzene

J. Brillo[a], A. Hammoudeh[c], H. Kuhlenbeck[a,*], N. Panagiotides[b], S. Schwegmann[b], H. Over[b], H.-J. Freund[b]

[a]*Fritz-Haber-Institut der Max-Planck-Gesellschaft, Abteilung Chemische Physik, Faradayweg 4–6, D-14195 Berlin, Germany*
[b]*Abteilung Physikalische Chemie, Faradayweg 4–6, D-14195 Berlin, Germany*
[c]*Yarmouk University, Faculty of Sciences, Department of Chemistry, Irbid, Jordan*

Received 11 May 1998; accepted 12 June 1998

Abstract

We report on studies dealing with the structure of WC(0001) and the adsorption of benzene on this surface. An *I(V)*-low-energy electron diffraction structure analysis has been performed to elucidate the surface structure of WC(0001). These studies indicate that the surface consists of a tungsten layer covered by carbon randomly distributed on the hcp sites with a coverage of 30% that of a full carbon layer. The distance between this carbon layer and the tungsten layer beneath is enlarged by 5% with respect to the spacing between carbon and tungsten layers in the bulk. Only a small deviation from the bulk value was found for the distance between the first tungsten layer and the carbon layer below. No indications of surface reconstruction have been observed. Benzene adsorption was studied on clear oxygen covered and oxidized WC(0001). The benzene multilayer desorbs at $T \leq 200$ K. On stoichiometric WC(00001), molecular benzene of (sub)monolayer coverage is found up to temperatures of $T \approx 230$ K. After desorption of this species, small signals of fragments are visible in the photoelectron spectra up to $T \approx 1000$ K. Above this temperature, a graphite covered surface remains. On a surface covered by a thin closed oxide phase (WO) only multilayer adsorption is found; above $T \approx 200$ K no adsorption takes place under UHV conditions. Weakly oxidized WC(0001) interacts more strongly with benzene in that strong photoemission signals of a (sub)monolayer species are visible up to a temperature of $T \approx 340$ K.

Keywords: Tungsten carbide; Oxygen; Angle resolved photoemission; Benzene; I(V)-LEED

1. Introduction

Tungsten carbide is a technologically important material. Since this compound is very hard, it is applied for coatings of tools. Its electronic and thermal properties are similar to those of metals, in that it is electrically conducting and exhibits high thermal conductivity. Due to a certain similarity of its electronic structure with that of platinum the idea came up that the catalytic properties could also be similar which might allow for a replacement of noble metals used in certain catalysts with this considerably cheaper material [1–4]. This idea triggered several studies on the catalytic properties of tungsten carbide [1–14]. It has been shown to catalyze isomerization, hydrogenation and dehydrogenation reactions [5–9]. It was also shown that the catalytic activity depends strongly on oxygen contaminations on the carbide surface [8, 11, 12]. There is still a discussion on the influence of the different oxygen species onto the catalytic activity [8, 11–13] although there are indications

* Corresponding author.

0368-2048/98/$ - see front matter
PII: S0368-2048(98)00222-9

that WO_2 at the surface is at least partly responsible [15, 16].

In order to learn about the interaction of surfaces with adsorbates, it is helpful to investigate well defined systems, i.e. to study adsorption on single crystals under UHV conditions. One prerequisite for an understanding of the data is the knowledge of the structure of the surface. There are no data available on this topic which is why we have performed an $I(V)$-low-energy electron diffraction (LEED) structure analysis.

Johansson et al. [17] have investigated the electronic structure of a WC(0001) single crystal and some data have been published on the adsorption of CO, NO and O_2 [18–21]. These papers demonstrate that stoichiometric WC(0001) interacts strongly with adsorbates. For the case of CO and NO, it was shown that the bonding of these adsorbates to the tungsten carbide is similar to that observed for transition metals like nickel, platinum, etc, which is not unexpected in view of the metal-like electronic structure of the carbide. Preadsorbed oxygen reduces the interaction strength for all studied adsorbates. The studies have also shown that a stoichiometric WC(0001) surface is hard to maintain. Under conditions as applied in catalysis, a non-stoichiometric surface, possibly covered by graphite, oxygen or other impurities, is more likely to exist than a stoichiometric and clean one.

2. Experimental

The WC(0001) single crystal has been cut from a tungsten carbide block after orientation with Laue backscattering. It contained appreciable amounts of iron which were removed by glowing the sample at $T \geq 2000$ K for 10 min. Thereafter, the sample was polished using standard procedures.

The crystal was mounted on a sample holder which allowed for temperature variation between $T \approx 90$ K and $T \geq 2500$ K. It was spotwelded to two tantalum wires ($\phi = 0.25$ mm) which were attached to two tungsten rods ($\phi = 1$ mm). These were plugged into a sapphire block which was in direct contact with a reservoir that could be filled with liquid nitrogen for cooling purposes. Heating was possible using a tungsten filament mounted behind the backside of the sample. The sample temperature was determined with a W–Re 26%/W–Re 95% thermocouple spotwelded to one of the tantalum wires at a point where the latter was in direct contact with the crystal.

The main impurity found during preparation of the sample was sulfur. This could be removed by prolonged annealing at elevated temperature ($T \geq 1300$ K) and sputtering. A major problem was the stoichiometry of the sample surface. The carbon/tungsten ratio was adjusted by annealing in an oxygen atmosphere ($P \approx 10^{-7}$ mbar, $T \approx 1300$ K) or sputtering if there was too much carbon on the surface, or by glowing in methane ($P \geq 5 \times 10^{-4}$ mbar, $T \geq 1300$ K) when the surface was carbon deficient. Graphitic carbon could be transformed into its carbidic state by prolonged glowing at $T \approx 1600$ K.

The UHV system used for the photoelectron experiments was attached to the TGM3 beamline at the BESSY electron storage ring in Berlin. It was equipped with a electron energy analyser rotatable in two orthogonal planes, allowing angular-resolved photoelectron spectroscopy to be performed. Thermal desorption spectra could be taken using a differentially pumped quadrupole mass spectrometer equipped with a so-called Feulner cup [22]. Apart from this, the system was equipped with facilities for sample preparation (ion bombardment gun) and surface characterization (Auger electron spectroscopy, LEED). The equipment of the system used for the $I(V)$-LEED experiments was similar but it did not contain an electron energy analyser.

LEED $I(V)$ data were recorded at normal incidence and a sample temperature of 295 K in the energy range from 50 to 335 eV. The measurement was performed on-line with a four-grid LEED optics and a computer-controlled video-LEED system similar to that described in Ref. [23], taking the integrated spot intensities in 1 eV steps from a fluorescent screen and automatically subtracting a linearly interpolated background intensity. Five non-equivalent integer order beams yielded a total energy range of 1240 eV. In order to check for normal incidence, at least two symmetrically equivalent beams were measured in each case; small deviations from normal incidence were compensated for by averaging [24]. The total measuring time was about 30 min; no effects of beam damage nor residual gas adsorption on the $I(V)$ data could be detected within the limits of accuracy. The experimental data were further smoothed

a) LEED-pattern of a stoichiometric WC(0001) surface. E_{kin}=61eV.

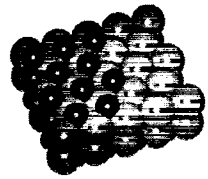

b) Ideal structure of tungsten and carbon terminated WC(0001). The small spheres represent carbon.

c) Non stoichiometric surface: C/W=1.1. E_{kin}=141 EV.

d) Non stoichiometric surface: C/W=0.75. E_{kin}=57 eV

Fig. 1. LEED patterns of stoichiometric and non-stoichiometric WC(0001). At the right-hand side (top), a structural model of the WC(0001) surface is shown.

MODEL (side view)		R_{Pendry}
1 C(1) : 100% W(1) : 0%		0.60
2 C(1) : 0% W(1) : 100%	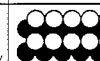	0.40
3 C(1) : 30% W(1) : 0%		C(1) on: hcp 0.36; fcc 0.46; bridge 0.44; top 0.59
4 C(1) : 30% W(1) : 70%		0.43
5 stacking fault		0.74
6 stacking fault		0.80
7 stacking fault		0.78

Fig. 2. Optimum Pendry R-factor for different models of the WC(0001) surface. The sketches show side views in the [10$\bar{1}$0] direction; carbon atoms are shaded. Models 1–4: different concentrations of C and W in the topmost layer; for model 3, in addition, the adsorption site of C in the topmost layer was varied. Models 5–7: possible stacking faults in the topmost three layers (only hollow sites are considered). In all cases the bulk stacking sequence 'abab' is maintained.

and divided by the energy dependent emission current before comparison with simulated data.

For the structural analysis on basis of this data set, full-dynamical LEED calculations were performed using the program package of Moritz [25]. Nine spin-averaged, relativistically corrected phase shifts were used to describe the electron scattering by the tungsten as well as by the carbon atoms (cf. Ref. [26, 27] for details); inelastic scattering was introduced by an imaginary part of the potential. Isotropic thermal vibrations were considered in the Debye approximation, taking the Debye temperatures of W and C as fitting parameters.

The agreement between experimental and simulated data was judged from Pendry's R-factor, R_{Pendry} [29]. The refinement of structural parameters, the real part of the muffin-tin zero and the Debye temperature were carried out using a non-linear least-squares optimization scheme based on the algorithm of Marquardt [29–31].

3. Results and discussion

3.1. Structural studies

A set of LEED patterns of stoichiometric and non-stoichiometric WC(0001) is shown in Fig. 1 together with a model of the surface. The stoichiometric surface displays a simple hexagonal LEED pattern (Fig. 1a) as expected for a non-reconstructed bulk-truncated WC(0001) surface (see Fig. 1b). However, this pattern gives no clue to the type of termination of the carbide at the surface. Fig. 1b illustrates that the first layer may consist either of tungsten or carbon or a mixture of both. The non-stoichiometric surfaces are characterized by more complex LEED patterns (see Fig. 1c and 1d). For the surface with a carbon/tungsten ratio of 1.1 which exhibits $(\sqrt{3}\times\sqrt{3})R30°$, one might expect that the additional carbon atoms occupy $(\sqrt{3}\times\sqrt{3})R30°$ positions at the surface whereas the pattern displayed in Fig. 1d may not be interpreted so easily.

In order to determine the atomic geometry of the stoichiometric surface exhibiting a simple (1×1)-pattern, a LEED intensity analysis was performed.

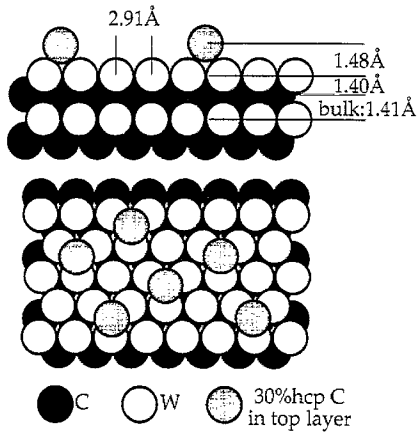

Fig. 3. Best fit model of the WC(0001) surface according to LEED $I(V)$ analysis. The surface is mainly tungsten terminated without stacking faults; 30% of the available hcp hollow sites are occupied by additional carbon atoms.

In a first step, only the two bulk-terminated models, which are shown in Fig. 2, models 1 and 2, were considered, the topmost two layer distances being the only structural fitting parameters. From these calculations, it becomes obvious that pure carbon termination at the surface Fig. 2, model 1, is not likely since the optimum R_{Pendry} is significantly larger than for the purely tungsten terminated model. Therefore, starting from this model, further structural details were taken into account.

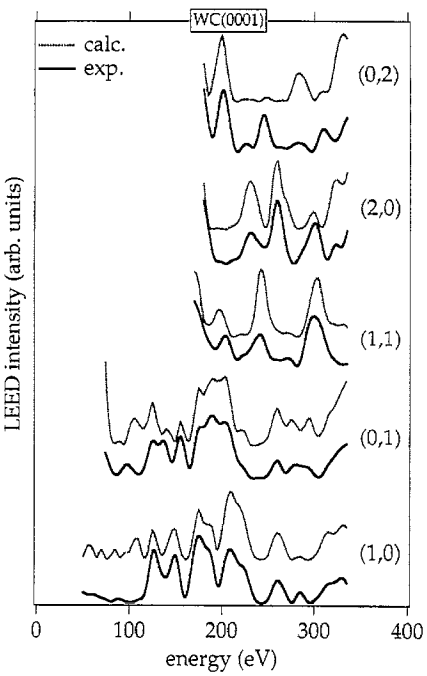

Fig. 4. Experimental $I(V)$ curves in comparison with corresponding simulated data for the optimum model which is shown in Fig. 3.

Two kinds of deviations from a bulk-terminated surface, which are compatible with the observed (1×1) LEED pattern, were tested in the fit. First there might be a 'stacking fault', i.e. the bulk 'abab' layer sequence could be broken at the surface. If one assumes that each layer occupies one kind of hollow site on the underlying layer and that the tungsten–carbide–tungsten layer sequence is maintained, there are three possible stacking faults of the topmost three layers for a tungsten terminated surface. For each of these configurations, the topmost layer distances were again optimized; the resulting optimum R_{Pendry} values are compiled in Fig. 2, models 5–7. In all cases, the R-factor is significantly larger than for the bulk-terminated model 2. So stacking faults can safely be excluded.

Second, a random distribution of additional atoms on the top layer in the form of a lattice gas or a random substitution of tungsten atoms by carbon (or vice versa) would also yield a (1×1) LEED pattern with only increased diffuse background intensity. For these simulations, the average t-matrix approximation was used [32], which describes multiple scattering between the randomly distributed atoms only in an averaged fashion. In this way, we introduced a variable carbon concentration in different sites on top of the tungsten terminated surface model (Fig. 2, model 3). Four high symmetry sites were tested (hcp and fcc hollow sites, twofold bridge site, top site); in each case, the carbon concentration and the C–W layer distance were optimized. Only for the model with carbon in hcp hollow sites could the R-factor be lowered; the optimum model concentration turned out to be 30% of a monolayer with $R_{\text{Pendry}} = 0.36$. For all other sites, an occupation factor of 0.30 increased the R-factor significantly in the sense of Pendry's RR-factor ($RR^{*}R_{\text{Pendry,min}} = 0.06$) [28]. This was also the case for a model where 30% of the tungsten atoms in the top layer are substituted by carbon (Fig. 2, model 4).

The optimum model according to our LEED $I(V)$ analysis is displayed in Fig. 3: 30% of the hcp hollow

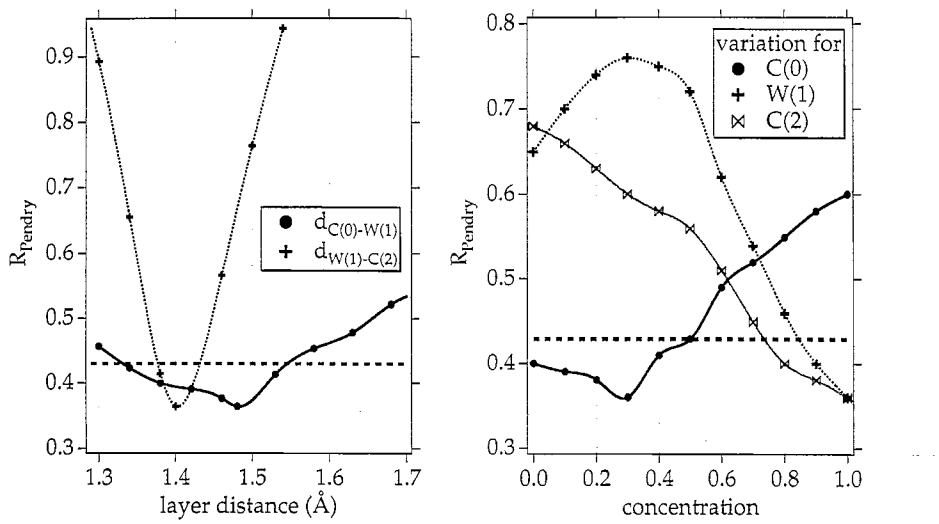

Fig. 5. Pendry R-factors for model 3 (hcp) of Fig. 2 as a function of the layer distances (left panel) and the occupation factors (right panel) of the topmost three layers C(0), W(1) and C(2). In each case, only one parameter is varied, keeping all the others fixed at their optimum values. The dashed line indicates the error bar according to Pendry's RR-factor.

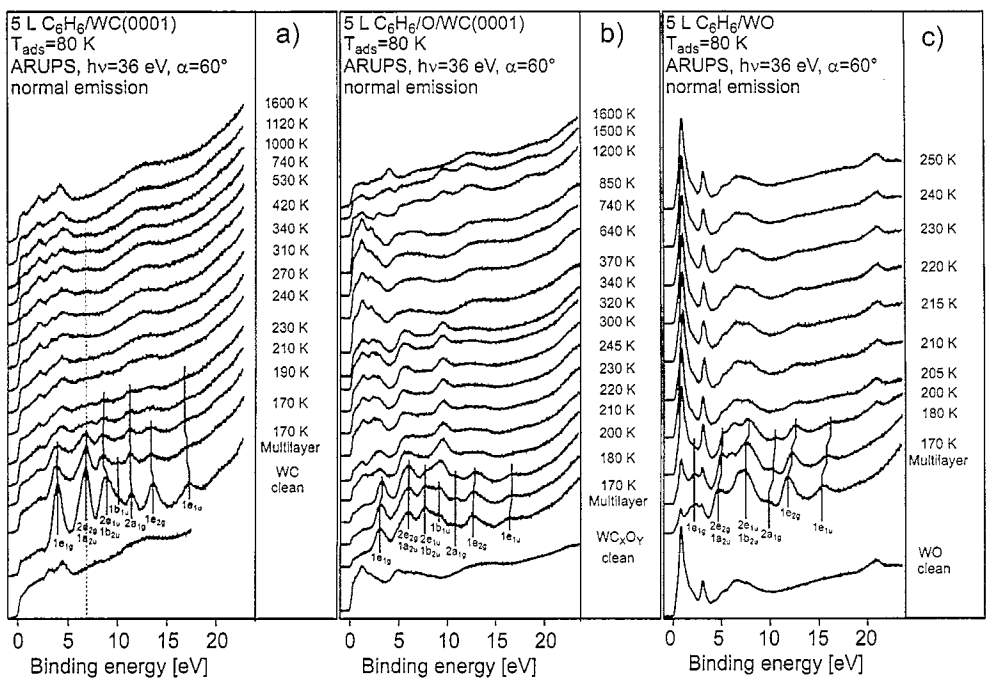

Fig. 6. ARUPS spectra of 5 l C_6H_6 on clean and oxygen dosed WC(0001). (a) C_6H_6/WC(0001), (b) C_6H_6/2000 l O_2 (T = 600 K)/WC(0001), (c) C_6H_6/2000 l O_2 (T = 900 K)/WC(0001).

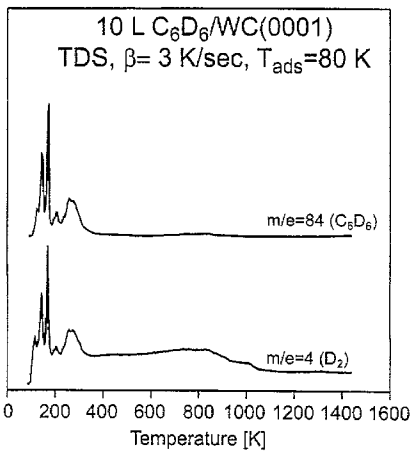

Fig. 7. Thermal desorption spectra of C_6D_6 on WC(0001) with the mass spectrometer set to mass 84 (C_6D_6) and 4 (D_2).

sites on an otherwise tungsten bulk-terminated surface are occupied by carbon. The distance between the partly occupied carbon layer and the underlying tungsten layer is expanded by 0.07 Å with respect to the bulk value; all deeper layer distances are almost bulk like. The corresponding $I(V)$ curves are shown in Fig. 4; although the Pendry R-factor of 0.36 is still relatively high if compared to typical analyses of clean metal surfaces, the general shapes of the curves and most peak positions are well reproduced by the simulation. The remaining discrepancies may be a result of an insufficient description of the disordered carbon layer.

In Fig. 5, the dependences of R_{Pendry} on the layer distances and on the concentrations of C respectively W in the topmost three layers are shown; in each case, all other parameters are fixed at their optimum values. From these plots, the error bars of the analysis for the layer distances and occupation numbers can be estimated [29]: the real values are within 6% probability in the range where the R-factor is lower than $(1 + RR)^* R_{\text{Pendry,min}} = 0.43$. Therefore, a purely tungsten terminated surface also cannot be excluded on the basis of the current $I(V)$ data.

4. Adsorption of benzene

Previously we have studied the adsorption of O_2, NO and CO on WC(0001) [20, 21]. These studies have shown that the adsorption properties of this carbide are similar to those of a reactive transition metal. In view of the catalytic activity of the surface for hydrogenation, dehydrogenation and isomerization reactions, we have investigated the interaction of the surface with benzene.

Fig. 6 displays spectra of C_6H_6 on clean and oxygen precovered WC(0001). The left panel (a) exhibits data for adsorption on clean WC(0001). For the data in panel (b), the substrate was pretreated with oxygen such that a mixture of WC, WO and oxycarbide or carbonate (WC_xO_y) formed [21], whereas panel (c) displays data for a surface covered with a layer of WO. In all three sets of spectra, multilayer adsorption of benzene is observed up to $T \approx 200$ K.

After desorption of the multilayer from clean WC(0001) (Fig. 6a), the benzene induced features vanish gradually. At temperatures above $T \approx 230$ K, only a small feature at about 7 eV remains which is marked by a dotted guide line in the data. It is visible up to temperatures of about $T \approx 1000$ K. The situation is different for the weakly oxidized surface (Fig. 6b). This surface exhibits a mixture of WC, WO and WC_xO_y [21]. Here, even after desorption of the benzene multilayer, strong adsorbate induced features are observed up to temperatures of $T \approx 340$ K. For the strongly oxidized surface (Fig. 6c), only multilayer adsorption is found; the small features which are visible at about 8 eV and 13 eV up to a temperature of about $T \approx 230$ K are likely to be attributed to traces of CO adsorbed from the residual gas. The weak interaction of benzene with the WO covered surface is in line with studies of CO adsorption [20, 33] which have shown that WO is rather inert.

Some additional information is supplied by the TDS spectra shown in Fig. 7. The data were collected for desorption of C_6D_6 and D_2 from WC(0001) dosed with deuterated benzene. At temperatures below $T =$ 200 K, features due to desorption of the multilayer show up (similar features have been observed for multilayer desorption from W(110) [34]) and at about 260 K another state is found which is to be attributed to desorption of molecular (sub)monolayer benzene. This desorption peak most likely corresponds to the disappearance of some peaks in Fig. 6a at $T \approx 230$ K. The discrepancy in temperatures may be due to the facts that the thermocouple used for temperature determination could not be spot-welded

directly to the sample and that we had to use a W/Re thermocouple which exhibits only small thermovoltages. Above 260 K, only D_2 desorption occurs indicative of dissociation of benzene or benzene fragments. The dissociation product is likely the one that leads to the small feature at about 7 eV in Fig. 6a and 6b. We attribute it to a fragment of benzene since it is unlikely that benzene exists molecularly on the surface up to temperatures in the region of $T \approx$ 1000 K which is about the temperature at which hydrogen desorption stops in Fig. 7. D_2 desorption occurs over a large temperature range in Fig. 7 and the desorption signal is structured, which most likely means that hydrogen loss occurs in several dehydrogenation steps. The observed binding energy of 7 eV in the photoelectron spectra would fit to a CH_x type species [35, 36]. According to Ref. [34], C–H bonds are found on the surface of W(110) even after annealing at temperatures in the range of $T \approx$ 1000 K. This is obviously also the case for the WC(0001) surface and may at least partly be traced back to the tungsten termination of the carbide surface. Auger spectra show that after hydrogen desorption, a graphite covered surface remains.

The influence of preadsorbed oxygen on a benzene adsorbate seems to be similar to that observed for CO [21] in that oxygen on the surface reduces the interaction strength. In the case of benzene, this means that on clean WC(0001) dissociation occurs, on a weakly oxidized surface, a chemisorbate and on a strongly oxidized surface, only multilayer adsorption is found.

The results are similar to those obtained for benzene adsorption on oxygen- and carbide-modified Mo(110) [37]. Benzene bonds only weakly to the oxygen-modified surface whereas dissociation occurs on the carbide modified surface at $T \approx$ 350 K. The dissociation products were identified to be of C_xH_y type.

5. Summary

With $I(V)$-LEED analysis, the structure of the WC(0001) surface has been characterized. The smallest R-factor was obtained for a tungsten terminated surface which is covered by carbon atoms randomly distributed on the hcp sites with the carbon coverage corresponding to 30% of that of a full carbon layer. However, a purely tungsten covered surface cannot be excluded on the basis of the present data.

Benzene adsorption on WC(0001) with and without oxygen precoverage was studied with TDS and ARUPS. The interaction depends strongly on the oxygen precoverage. A strongly oxidized surface which exposes only WO to the adsorbate shows only multilayer adsorption; no evidence of a benzene monolayer could be found. For a weakly oxidized surface which exposes a mixture of WC, WO and oxycarbide or carbonate, a benzene monolayer signal is found up to a temperature of $T \approx$ 340 K in the photoemission data. On clean WC(0001), benzene dissociation is observed, leading to species on the surface which are most likely at least partly of CH_x type. Upon warming up, the fragments lose hydrogen until at $T \approx$ 1000 K a graphite covered surface remains.

Acknowledgements

This work has been funded by the Bundesministerium für Forschung und Technologie under contract number 05 625 PCA 3. We acknowledge Prof. A. Katrib and Prof. G. Maire for helpful discussions as well as Dr Görting who supplied us with the tungsten carbide single crystal.

References

[1] R.J. Colton, J.-T.J. Huang, J.W. Rabalais, Chem. Phys. Lett. 34 (1975) 337.
[2] R.L. Levy, M. Boudart, Science 181 (1973) 547.
[3] S.T. Oyama, The Chemistry of Transition Metal Carbides and Nitrides, Blackie, Glasgow, 1996.
[4] L. Leclerq, M. Provost, G. Leclerq, J. Catal. 117 (1989) 384.
[5] J.M. Muller, Gault, F. G., Bull. Soc. Chim. Fr., 2 (1970) 416.
[6] V. Keller, P. Wehrer, F. Garvin, R. Ducros, G. Maire, J. Catal. 153 (1995) 9.
[7] V. Keller, P. Wehrer, F. Garin, R. Ducros, G. Maire, J. Catal. 166 (1997) 125.
[8] F. Garin, V. Keller, R. Ducros, A. Muller, G. Maire, J. Catal. 166 (1997) 136.
[9] I. Kojima, E. Miyazaki, J. Catal. 89 (1984) 168.
[10] K.E. Curry, L.T. Thompson, Catalysis Today 21 (1994) 171.
[11] M. Muller, V. Keller, R. Ducros, G. Maire, Catal. Lett. 34 (1995) 65.
[12] V. Keller, M. Cleval, F. Maine, P. Wehrer, R. Ducros, G. Maire, Catalysis Today 17 (1993) 493.
[13] E.K. Curry, L. Thompson, Symposium on Chemistry and

Characterization of Supported Metal Catalysts, 206th National Meeting of the American Chemical Society, 1993, p. 877.
[14] A. Katrib, F. Hemming, L. Hilaire, P. Wehrer, G. Maire, J. Electron Spectrosc. Relat. Phenom. 68 (1994) 595.
[15] A. Katrib, F. Hemming, P. Wehrer, L. Hilaire, G. Maire, J. Electron Spectrosc. Relat. Phenom. 76 (1995) 195.
[16] A. Katrib, V. Logie, N. Saurel, P. Wehrer, L. Hilaire, G. Maire, Surf. Sci., 377–379 (1997) 754.
[17] P.M. Stefan, M.L. Shek, I. Lindau, W.E. Spicer, L.I. Johansson, F. Hermann, R.V. Kasovski, G. Brogen, Phys. Rev. B 29 (1984) 5423.
[18] K.L. Hakanson, H.I.P. Johansson, L.I. Johansson, Phys. Rev. B 49 (1994) 2035.
[19] P.M. Stefan, Ph.D. thesis, University Stanford, 1983.
[20] J. Brillo, R. Sur, H. Kuhlenbeck, H.-J. Freund, Surf. Sci. 397 (1998) 137.
[21] J. Brillo, H. Kuhlenbeck, H.-J. Freund, Surf. Sci. 409(2) (1998) 199.
[22] P. Feulner, D. Menzel, J. Vac. Sci. Technol. A 17 (1980) 662.
[23] P. Heilmann, E. Lang, K. Heinz, K. Müller, in P.M. Marcus, F. Jona (Eds.), Determination of surface structures by LEED, Plenum Press, New York, 1984, p. 463.
[24] H.L. Davis, J.R. Noonan, Surf. Sci. 115 (1982) L75.
[25] W. Moritz, J. Phys. C. 17 (1983) 353.
[26] H. Over, H. Bludau, M. Skottke-Klein, G. Ertl, W. Moritz, C.T. Campbell, Phys. Rev. B 45 (1992) 8638.
[27] H. Over, T. Hertel, H. Bludau, S. Pflanz, G. Ertl, Phys. Rev. B, 48 (1993) 5572, see also references cited therein.
[28] J.B. Pendry, J. Phys. C 13 (1980) 937.
[29] D.W. Marquardt, J. Soc. Indust. Appl. Math. 11 (1963) 431.
[30] G. Kleinle, W. Moritz, G. Ertl, Surf. Sci. 238 (1990) 119.
[31] H. Over, U. Ketterl, W. Moritz, G. Ertl, Phys. Rev. B 46 (1992) 15438.
[32] F. Jona, K.O. Legg, H.D. Shih, D.W. Jepsen, P.M. Marcus, Phys. Rev. Lett 40 (1978) 1466.
[33] J. Brillo, R. Sur, H. Kuhlenbeck, H.-J. Freund, J. Electron Spectrosc. Relat. Phenom., 88–91 (1998) 809.
[34] J.E. Whitten, R. Gomer, Surf. Sci. 347 (1996) 280.
[35] F. Solymosi, I. Kovacs, K. Révész, Surf. Sci. 356 (1996) 121.
[36] N. Schühler, P. Oelhafen, Surf. Sci. 365 (1996) 817.
[37] J. Eng, B.E. Bent, B. Frühberger, J.G. Chen, J. Phys. Chem. B 101 (1997) 4044.